Advanced Composite Materials
Publication details, including instructions for authors and subscription information:
http://www.tandfonline.com/loi/tacm20

Vibration Analysis of Multiple Delaminated Composite Beams

Hasan Çallioğlu [a] , Gökmen Atlihan [a] & Muzaffer Topçu [a]

[a] Department of Mechanical Engineering, Pamukkale University, 20017 Denizli, Turkey

Version of record first published: 17 Jul 2012.

///VSP///
Advanced Composite Materials 21 (2012) 11–27
ADVANCED COMPOSITE MATERIALS
brill.nl/acm

Vibration Analysis of Multiple Delaminated Composite Beams

Hasan Çallioğlu, Gökmen Atlihan * and Muzaffer Topçu
Department of Mechanical Engineering, Pamukkale University, 20017 Denizli, Turkey

Received 8 June 2011; accepted 13 October 2011

Abstract
In this study, the effects of location, size and number of delaminations, boundary conditions, orientation angles and stacking sequences on the natural frequency of laminated composite beams are investigated experimentally, analytically and numerically. Two-dimensional finite element models of the delaminated beams are obtained using ANSYS (Finite Element Method Code). The analytical method is developed using Euler–Bernoulli beam theory. Then, analytical results are compared with the results available in the literature and the numerical and experimental results in the present study. It has been seen that all results obtained are very close to each other. It is shown that the natural frequencies decrease when sizes and numbers of edge and middle delaminations in the beam increase, and the location of the delamination is also very important. The first natural frequency value of beam of $[0°/90°]_8$ is found to be the highest as compared to the beams with angles $[30°]_{16}$ and $[60°]_{16}$. However, the natural frequency values in the beams that have the angle-ply of $[\theta]_{16}$ are lower than those of $[\theta/-\theta]_8$, $[(\theta/-\theta)_4]_s$ and $[(\theta/-\theta)_s]_4$.

Keywords
Natural frequency, vibration, FEM, experimental analysis, analytical analysis, delamination

1. Introduction

Composite materials offer the user many beneficial features, such as high strength and stiffness to weight ratios, which make them particularly suited to develop load bearing components for a variety of applications of the aerospace, naval and aeronautical industries. Some features such as strength, toughness, specific weight, corrosion and wear resistance and thermal features can be developed by the formation of a composite material and orienting fibers in proper directions.

* To whom correspondence should be addressed. E-mail: gatlihan@pau.edu.tr
Edited by the KSCM.

DOI:10.1163/156855111X614538

While composite materials have these advantages, they are also prone to a wide range of defects and damage which may significantly reduce their structural integrity. Interlaminar cracking or delamination, probably the most frequent kind of damage in composite laminates, occurs due to weak interlaminar strength. Delamination may arise either as a result of imperfect fabrication processes, such as incomplete wetting and entrapped air pockets between layers, or as a result of certain in-service factors, such as low velocity impact by foreign objects, for instance, dropped tools or bird strikes.

Although delamination damage is known to cause a degradation of overall stiffness and strength of the laminates, how many delaminations cause a change in vibration characteristics has already been investigated. The delaminated sublaminate generally exhibits new vibration modes and frequencies that depend on the number, size and location of the delamination. In particular, delaminations reduce the natural frequency, which may cause resonance if the reduced frequency is close to the working frequency. It is imperative that we should be able to predict the changes in the frequency, as well as the mode shape, in a dynamic environment.

As a result, the location, size and number of delaminations in laminated composite beam or plate affect the natural frequency and they are crucial from this point of view. Vibrations of the laminated composite plates and beams without delamination can be found in the literature [1–3].

In the literature, there are some studies on the vibration of the laminated composite beams having single and multiple delaminations. Alnefaie [4] developed a three-dimensional (3D) finite element model of delaminated fiber-reinforced composite plates for dynamics analysis. This model was used for detecting delaminations in composite plates. Ramtekkar [5] proposed two models — the unconstrained-interface model and the contact-interface model — for the computation of frequencies and the mode shapes of delaminated beams. Palacz *et al.* [6] presented a spectral finite element model for analysis of flexural-shear coupled wave propagation in delaminated multilayered composite beams. Chakraborty [7] performed an approach in predicting the presence of embedded delaminations in fibre-reinforced plastic composite laminates using natural frequencies as indicative parameters and an artificial neural network as a learning tool. Kumar and Shrivastava [8] developed a finite element formulation based on Higher Order Shear Deformation Theory and Hamilton's principle for the free vibration response of thick square composite plates having a central rectangular cutout, with and without the presence of a delamination around the cutout. Radu and Chattopadhyay [9] used a refined higher order shear deformation theory for the dynamic instability associated with composite plates with delamination under dynamic compressive loads. Luo and Hanagud [10] presented a new model that takes into account shear effect and rotary inertia for composite beams with through-width delaminations. Della and Shu [11, 12] developed analytical solutions for the free vibrations of multiple delaminated beams under axial compressive loadings using the Euler–Bernoulli beam theory. Kim *et al.* [13] used a dynamic analysis method to investigate and characterize the effect of the presence of discrete single and multiple embedded delaminations on the dynamic response of laminated composite structures with balanced/unbalanced. Lee *et al.* [14] proposed an analytical formulation derived from the assumption of constant curvature at the multi-delamination for free vibration analysis of multi-delaminated composite beams. Lee [15] presented free vibration analysis for a laminated beam with delamination using a layerwise theory. He derived equations of motion from Hamilton's principle, and developed a finite element method to formulate the problem.

Some researchers have also shown the effects of stacking sequences on natural frequencies of laminated composite beams. Topcu *et al.* [16] studied the effects of stacking sequences on natural frequencies of laminated composite beams by using both experimental and theoretical approaches. Atlihan *et al.* [17, 18] investigated the effects of stacking sequences on natural frequencies of laminated composite beams *via* the Differential Quadrature Method (DQM). They demonstrated that the effective stiffness of the laminated composite beam can be altered through a change in the stacking sequence.

In this study, vibration behaviors of laminated composite beams having various delaminations, orientation angles, stacking sequences and boundary conditions are investigated experimentally, analytically and numerically. Single and multiple (two) delaminated composite beams are established for experimental proposes. ANSYS commercial program is used for a numerical solution (FEM method), and single and multiple delaminated models for the laminated composite beam have also been formed using ANSYS. The numerical and analytical results are compared with experiment results and they are found to be consistent. The analytical method is also compared with numerical, analytical and experimental methods available in the literature.

2. Free Vibration Analysis

2.1. Analytical Method

The bending moment M on a laminated composite beam shown in Fig. 1 can be written as [16]:

$$M = \frac{2b}{3\rho} \sum_{j=1}^{m/2} (E_x)_j \left(z_j^3 - z_{j-1}^3\right), \tag{1}$$

where b is width of the beam, ρ curvature of the beam, m the number of layers and z_j the distance between the outer face of jth layer and the neutral plane, respectively. The relationship between the bending moment and the curvature can be written as follows:

$$M = \frac{E_{\mathrm{ef}} I_{yy}}{\rho} = E_{\mathrm{ef}} I_{yy} \frac{\mathrm{d}^2 w}{\mathrm{d}x^2} \tag{2}$$

and

$$E_{\mathrm{ef}} = \frac{8}{h^3}\sum_{j=1}^{m/2}(E_x)_j\left(z_j^3 - z_{j-1}^3\right), \tag{3}$$

where E_{ef} is the effective elasticity modulus and I_{yy} is the cross-sectional inertia moment about the neutral axis of the beam.

The rate of change of shear along the length of the beam is equal to the loading per unit length, and the rate of change of the moment along the beam is equal to the shear [19]

$$\frac{\mathrm{d}^2 M}{\mathrm{d}x^2} = \frac{\mathrm{d}V}{\mathrm{d}x} = q(x), \tag{4}$$

where V represents shear force and $q(x)$ represents load in unit length. By substituting equation (2) into equation (4), the following equation can be obtained

$$\frac{\mathrm{d}^2}{\mathrm{d}x^2}\left(E_{\mathrm{ef}} I_{yy}\frac{\mathrm{d}^2 w}{\mathrm{d}x^2}\right) = q(x). \tag{5}$$

Equation (5) gives an expression for the beam exposed to static loading. Regarding dynamic loading, d'Alembert's principle is used where mass and acceleration terms are added to the expression above [2] to give

$$E_{\mathrm{ef}} I_{yy}\frac{\partial^4 w(x,t)}{\partial x^4} = q(x,t) - \frac{\rho_m A\,\partial^2 w(x,t)}{\partial t^2}, \tag{6}$$

where w and q become functions of time and domain. Thus, derivatives become partial derivatives where ρ_m is the mass density of the beam material and A is the beam cross-sectional area.

The natural frequency of the beam is a function of the material properties and the geometry. Therefore, they are not affected by the forcing functions; it means that for this study $q(x,t)$ can be taken as zero. Thus, equation (6) becomes

$$E_{\mathrm{ef}} I_{yy}\frac{\partial^4 w}{\partial x^4} + \rho_m A\frac{\partial^2 w}{\partial t^2} = 0. \tag{7}$$

To solve equation (7), separation of variables can be used for harmonic free vibration:

$$w(x,t) = \sum_{n=1}^{\infty} A_n \sin\frac{n\pi x}{L}\cos\omega_t t, \tag{8}$$

where ω_n is the frequency, A_n is amplitude of the beam and L is the length of beam. Substitution of this solution into equation (7) eliminates the time dependency and frequency ω_n can be obtained as below

$$\omega_n = \frac{\lambda}{L^2}\sqrt{\frac{E_{\mathrm{ef}} I_{yy}}{\rho_m A}}, \tag{9}$$

where λ is the dimensionless frequency parameter that can be calculated by using boundary conditions [18].

Due to the presence of the delamination in the beam, the reduction in stiffness of the beam may make it unsafe even if fracture does not occur, and would lead to an undesirable increase in the deflection of the beam under a load. In the case where the laminated composite beam has any delamination at other positions, i.e., strip-single and -multiple, edge and middle types.

The following equations can be derived from the 'rule of mixtures' formula [3]:

$$E_{\mathrm{zd}} = \frac{\sum_{i=1}^{m} E_{\mathrm{ef}} z_i}{z}, \tag{10}$$

$$E_{\mathrm{d}} = (E_{\mathrm{zd}} - E_{\mathrm{ef}}) \frac{A_{\mathrm{d}}}{A_{\mathrm{t}}} + E_{\mathrm{ef}}, \tag{11}$$

where E_{zd} is longitudinal Young's modulus of a laminate totally delaminated along one or more interfaces (imperfect effective elasticity modulus); m, the number of sublaminates formed by the delamination; z_i, the thickness of the ith sublaminate; E_{d}, the longitudinal Young's modulus of a laminate partially delaminated along one or more interfaces (imperfect effective elasticity modulus); A_{d}, the delaminated area; and A_{t} is the total interfacial areas.

When the composite beams have total or partial delaminations, E_{zd} in equation (10) or E_{d} in equation (11) can be used instead of the effective elasticity modulus E_{ef} in equation (9).

2.2. Finite Element Model for Delaminated Composites

The beam is constituted in the commercial package ANSYS 10.0 [20]. Initially the beams are modeled in order to get an initial estimation of the undamped natural frequencies, ω_n, and mode shape, n. Element type of Shell 99 may be used for layered applications of a structural shell model. The element has six degrees of freedom at each node; translations in x, y and z directions and rotations about x, y and z axes. This element is constituted by layers that are designated by numbers (LN — Layer Number), increasing from the bottom to the top of the laminate; the last number quantifies the existent total number of layers in the laminate (NL — Total Number of Layers). Thus, the model of the laminated composite beam is generated using sixteen layers. Table 1 gives the geometry and material properties of the laminated beams used. The geometry and boundary conditions of the laminated composite beam have been shown in Fig. 1.

The boundary conditions have been applied on the nodes in the y–z plane in which the origin of the axes is located. The degrees of freedom of all nodes about the y–z plane, which include displacements and rotations, are taken as zero. The dimensions of the beams in the x and y coordinates are $L = 400$ and $b = 20.5$ mm.

Figure 2 shows the positions of the edge and middle single delaminations. Figure 3 shows laminated composite beams having edge or middle delaminations, which consist of three or four areas.

Table 1.
Material properties and dimensions of the laminated composite beam

Properties	Symbol	Present	[21–25]
Longitudinal elasticity modulus	E_1 (MPa)	44 150	134 000
Transverse elasticity modulus	E_2 (MPa)	12 300	10 300
Shear modulus	G_{12} (MPa)	4096	5000
Poisson's ratio	ν_{12}	0.2	0.33
Density	ρ (kg/m^3)	2026	1480
Length	L (m)	0.400	0.127
Height	h (m)	0.0033	0.0127
Width	b (m)	0.0205	0.00102

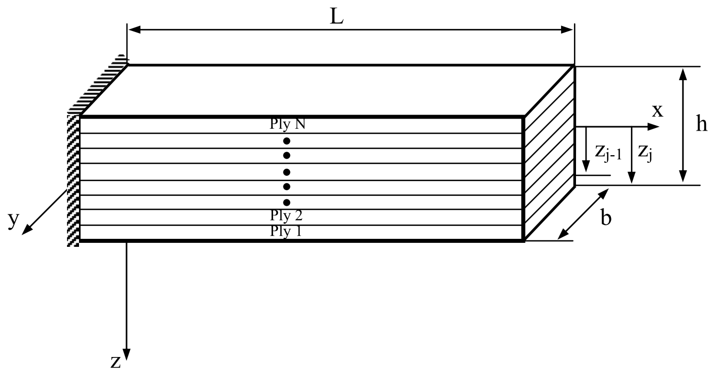

Figure 1. A laminated composite beam.

Figure 2. Positions of the single delaminations; (a) edge and (b) middle delamination types. This figure is published in color in the online version.

In the beams with edge delamination, area A1 is glued with areas A2 and A3, but the interface of A2 and A3 is not glued. Glue is a command in the ANSYS software program that is applied only to cases in which the intersection between entities occurs at a boundary, and is satisfied connected at their intersection. The entities maintain their individuality. In the same way, for the beams that have the middle delamination, areas A1 and A4 are glued with areas A2 and A3, individually. So, delamination has been formed between A2 and A3, as seen in Fig. 3. The double areas occur at the same coordinates of the interfacial areas when areas are meshed.

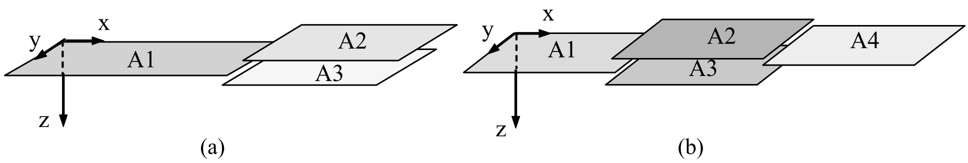

Figure 3. Laminated composite beams with (a) edge and (b) middle delaminations. This figure is published in color in the online version.

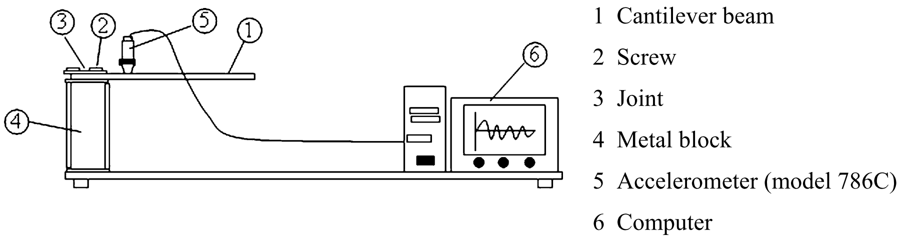

Figure 4. Experimental setup for the vibration measurement of the laminated composite beam.

Thus, the laminated composite beams have both edge and middle delaminations. In the same manner, edge and middle multiple delaminations can also be considered.

2.3. Experimental Natural Frequency Analysis

Figure 4 shows a laminate specimen clamped at one end using a joint fixed to a metal block using screws. The other end of the specimen is free to vibrate. A Wilcoxon Research accelerometer, Model 786C, is magnetically mounted close to the fixed side on a metal piece glued to the laminate specimen. The weight of the accelerometer may be considered high compared to the weight of the specimen. To reduce the effect of the weight on the measurements, the accelerometer is positioned near the fixed end of the beam. Data captured by the accelerometer is transferred through a power-amplifier unit to the Advantech X data acquisition card installed in a personal computer. A computer program developed specifically for these vibration experiments is used to receive vibration data from the data acquisition card, and to save it in a text file for later use.

The frequency for the laminate specimen $[45°]_{16}$ is calculated as follows using the data obtained from the accelerometer. It was measured that the time elapsed was $t = 236.2318$ ms while taking 1024 samples. Therefore the time interval elapsed is

$$\Delta t = \frac{236.2318}{1024} = 0.230535117 \text{ ms.}$$

The number of samples in one period is $k_\text{p} = 553$ as can see from Fig. 5. The time interval elapsed for one period is

$$\Delta t_\text{p} = \Delta t \cdot k_\text{p} = 0.230535117 \times 553 = 127.5743498 \text{ ms.}$$

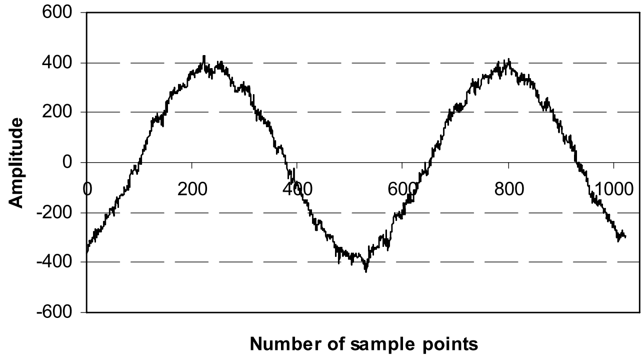

Figure 5. Vibration graphics of the laminated composite beam.

The frequency is

$$f = \frac{1000}{\Delta t_{\mathrm{p}}} = \frac{1000}{127.5743498} = 7.8385\ \text{Hz [26]}.$$

The natural circular frequency in radians per unit time for mode 1 ($n = 1$) is given as follows [16]:

$$\omega_n = \frac{\lambda}{L^2}\sqrt{\frac{E_{\mathrm{ef}} I_{yy}}{\rho_m A}} \tag{12}$$

and

$$f = \frac{\omega_n}{2\pi}. \tag{13}$$

The theoretical result is 8.0401 Hz.

3. Results and Discussion

In this study, vibration behaviors of laminated composite beams having edge and middle, single and multiple delaminations are investigated experimentally, analytically and numerically. Material properties and dimensions of the laminated composite beam are given in Table 1. Material properties of glass fiber reinforced epoxy matrix laminated composites (GFRP) were used in the present study; the other material properties are used for comparison with the studies in the literature. The orientation angles of the beams are chosen as $[30°]_{16}$, $[60°]_{16}$ and $[0°/90°]_8$, and single and multiple (e.g., two) delaminated composite beams, which have a strip type of delamination, are built up for experimental analysis. In the same way, the ANSYS commercial program is used for numerical solution (FEM method). Single and two delaminated models for the laminated composite beam are obtained and the effects of stacking sequences on the natural frequencies of the composite beams are investigated.

In analytical solution, Euler–Bernoulli hypothesis is valid and in the calculation of the natural frequency, the effective elasticity modulus E_{ef} for a non-delaminated beam or imperfect effective elasticity modulus E_d for a delaminated beam is used instead of elasticity modulus E in a beam made of isotropic material.

Single and two delaminated composite beams are produced for experimental analysis. During the manufacturing process, a Teflon film was put into the interlayer of the composite plates to give delamination in experimental analysis. The composite beams are of different delamination lengths. In single delaminated models, delamination is only between the middle layers while for two delamination models, delaminations are in the fourth layers from the top and bottom surfaces, as seen in Fig. 6(a) and (b).

In the same way, the finite element models for the laminated beams that have sixteen layers are obtained using finite element software program ANSYS 10.0 for various location, size and number of delamination. Two-dimensional finite element models of the laminated beams with single and multiple delaminations have also been established using ANSYS.

The natural frequency values obtained from analytical method are compared with the values presented in [21–25], as seen in Table 2. Figure 7 shows the geometry of a $[0°/90°]_{2s}$ cantilever beam and definition of damage cases which are utilized in Table 2. The frequency values are also quite close to each other. The minor differences among data are due to the use of Euler–Bernoulli beam theory in the analytical

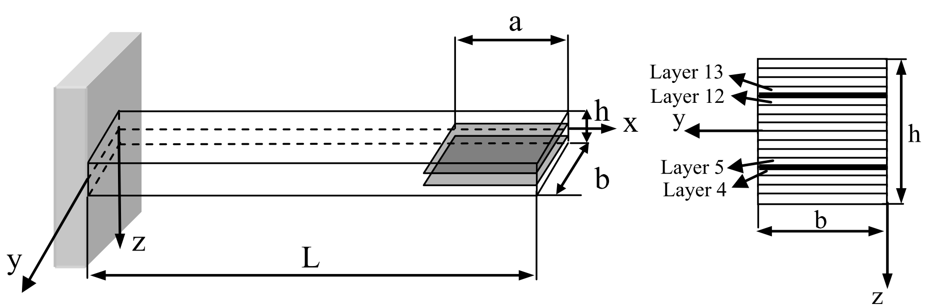

(a)

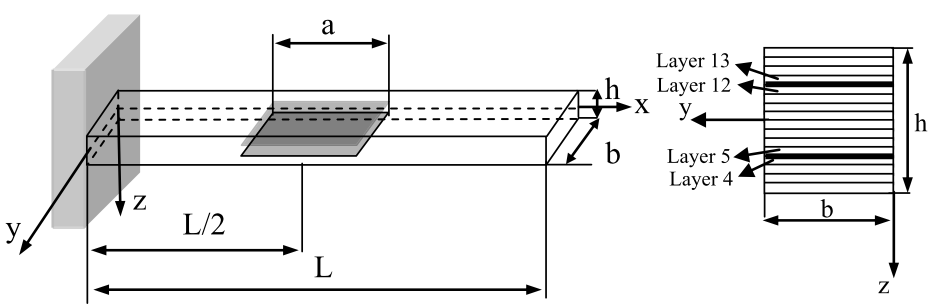

(b)

Figure 6. Positions of the two delaminations; (a) edge and (b) middle delamination types. This figure is published in color in the online version.

Table 2.
Comparison of natural frequencies of a cantilever delaminated beam

Del. length a (mm)	FEM [21] (Hz)	Mindlin FE [22, 23] (Hz)	Analytical [24] (Hz)	Experimental [25] (Hz)	Present (analytical) (Hz)
Intact 0.0	81.870	82.000	81.860	80.087	81.995
Case 1 50.8	76.522	76.643	76.807	75.369	73.422
Case 1 101.6	56.556	56.728	56.953	57.542	63.585
Case 2 50.8	76.889	77.013	76.621	75.126	75.681
Case 2 101.6	57.687	57.872	59.335	48.335	58.602
Case 3 50.8	80.451	80.564	80.740	79.750	77.787
Case 3 101.6	71.212	71.437	71.727	72.460	73.339
Case 4 50.8	80.620	80.736	80.867	68.917	80.010
Case 4 101.6	72.717	72.949	69.435	55.626	71.787

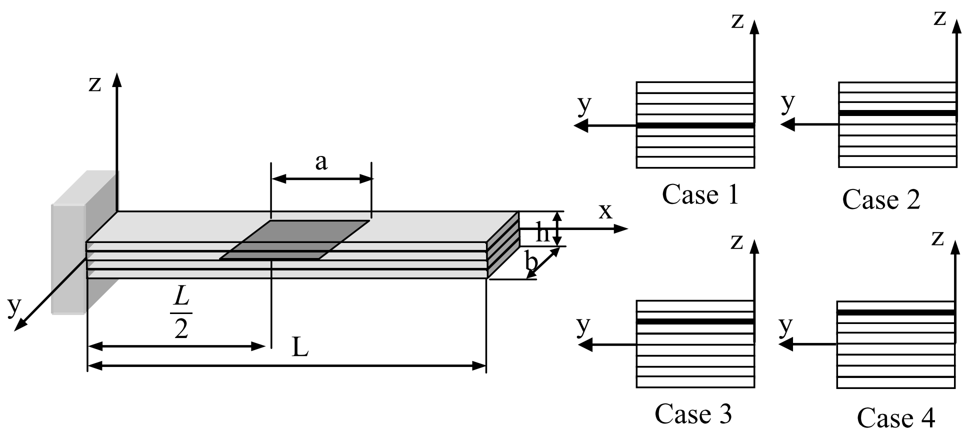

Figure 7. Geometry of a $[0°/90°]_{2s}$ cantilever beam and definition of damage cases. This figure is published in color in the online version.

model for the present study and Timoshenko beam theory or Mindlin plate theory in the others.

Figure 8 demonstrates variation of the first frequency with relative delamination length (a/L) for laminated composite beam having $[30°]_{16}$ of single-edge

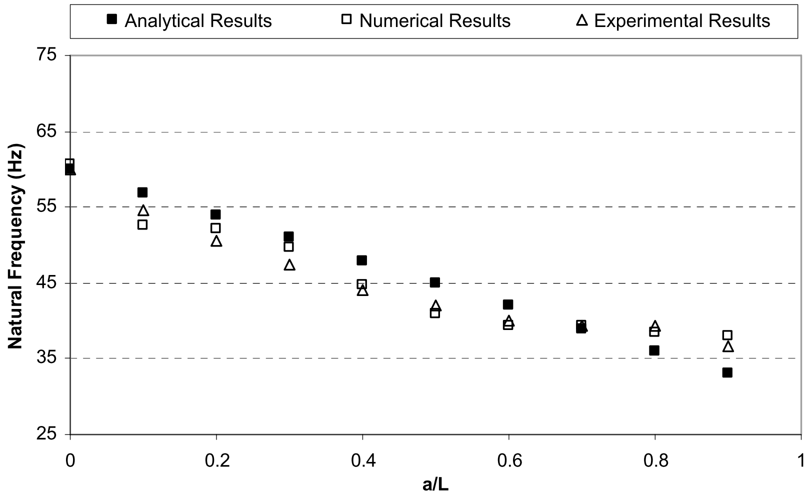

Figure 8. Variations of the frequency of $[30°]_{16}$ composite beam with single edge delaminations for clamped–clamped boundary condition.

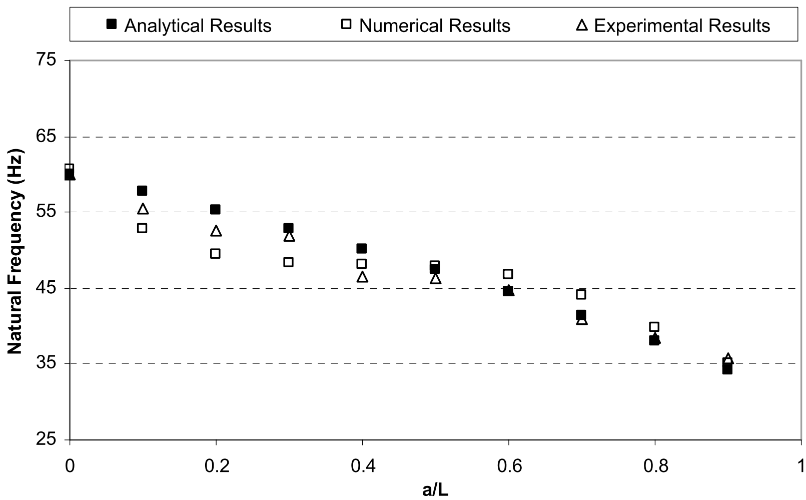

Figure 9. Variations of the frequency of $[30°]_{16}$ composite beam with single middle delaminations for clamped–clamped boundary condition.

delamination by using numerical, analytical and experimental results for clamped–clamped boundary condition. Here, a represents delamination length of the beam. While the delamination length in the composite beams increases, the frequency values decrease for all numerical, analytical and experimental data.

Figure 9 shows variation of the frequency *versus* the delamination length for laminated composite beam having $[30°]_{16}$ of single-middle delamination by using numerical, analytical and experimental results for clamped–clamped boundary condition. With increasing delamination length, the frequency values of the composite beams decrease. It is seen from the numerical results in Figs 8 and 9 that frequency values in beams having single-middle delamination are higher than those in beams having single-edge delamination when a/L ratio is between 0.34 and 0.85, and the values are equal to each other until the ratio is about equal to 0.11.

Although the results are very close to each other, the minor differences among the three methods arise from the assumption that the FEM model has a perfectly smooth surface and owing to the shear rotational effects are taken into account in the interlaminar regions of the beam. It is also extremely difficult to get a perfectly smooth surface in the material used in the experiments, and the shear and rotational effects do not take this into account in the interlaminar regions for which the Euler–Bernoulli hypothesis is valid.

Figure 10 shows variation of the frequency with delamination length (a/L) for laminated composite beam having $[30°]_{16}$ of multiple-edge delamination by using numerical, analytical and experimental results for clamped–clamped boundary condition. While delamination length in the composite beams increases, the frequencies values decrease for all methods. When the beams with multiple-edge delamination (Fig. 10) are compared with the beams of the single-edge delamination (Fig. 8), the frequency values of the beam with multiple-edge delamination are lower than those of the beams with single-edge delamination for all (a/L) ratios. The variations of the values are parallel to each other.

Figure 11 shows variation of the frequency *versus* the delamination length for laminated composite beam that has $[30°]_{16}$ of multiple-middle delamination for clamped–clamped boundary condition. With the increasing length and numbers of the delaminations in the composite beams, the frequency values decrease for all methods. It is seen that variation of the frequency values in the beams having

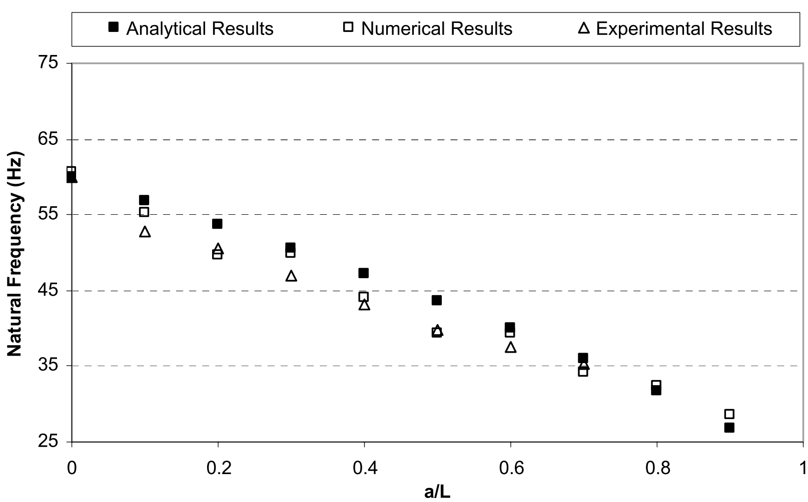

Figure 10. Variations of the frequency of $[30°]_{16}$ composite beam with multiple edge delaminations for clamped–clamped boundary condition.

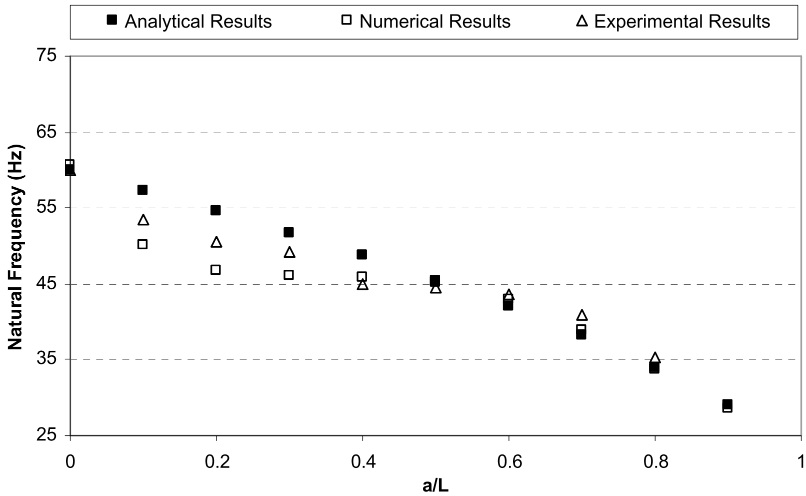

Figure 11. Variations of the frequency of $[30°]_{16}$ composite beam with multiple middle delaminations for clamped–clamped boundary condition.

multiple-middle delamination (Fig. 11) and multiple-edge delamination (Fig. 10) show similar trends to those of the single-middle (Fig. 9) and single-edge delamination (Fig. 8). The variations of the frequency values for multiple-middle and single-middle delaminated beams are parallel to each other.

Figure 12 shows the effect of the orientation angle on the natural frequency of a composite beam. The natural frequency values in the beams, which has clamped–clamped boundary condition and single-edge delamination, composed of angle-ply of $[30°]_{16}$ and $[60°]_{16}$ and cross-ply $[0°/90°]_{4s}$ are near to each other for the three methods. With increasing delamination length, the frequency values decrease gradually. The frequency values of the cross-ply beams of $[0°/90°]_{4s}$ are the highest when they are compared with those of the angle-ply beams.

Figure 13 shows the effect of boundary conditions on the natural frequency of a composite beam having single-edge or multiple-edge delamination. The frequency values are equal to each other for numerical and experimental results until an a/L ratio of about 0.3; after that, the frequency values of the beams with multiple-edge delamination decrease very much in comparison with the beams with single-edge delamination. As expected, the frequency values of the beams having clamped–clamped boundary conditions are higher than those of the beams having clamped–free boundary conditions.

Figure 14 shows the effect of the stacking sequence on the natural frequency values of the beams, which have clamped-free boundary condition and single-edge delamination ($a/L = 0.1$), composed of angle-ply of $[\theta]_{16}$, $[\theta/{-\theta}]_8$, $[(\theta/{-\theta})_4]_s$ and $[(\theta/{-\theta})_s]_4$ by using the numeric method. The natural frequency values in the beams that have angle-ply of $[\theta/{-\theta}]_8$, $[(\theta/{-\theta})_4]_s$ and $[(\theta/{-\theta})_s]_4$ are approximately similar to each other. However, the natural frequency values in the beams

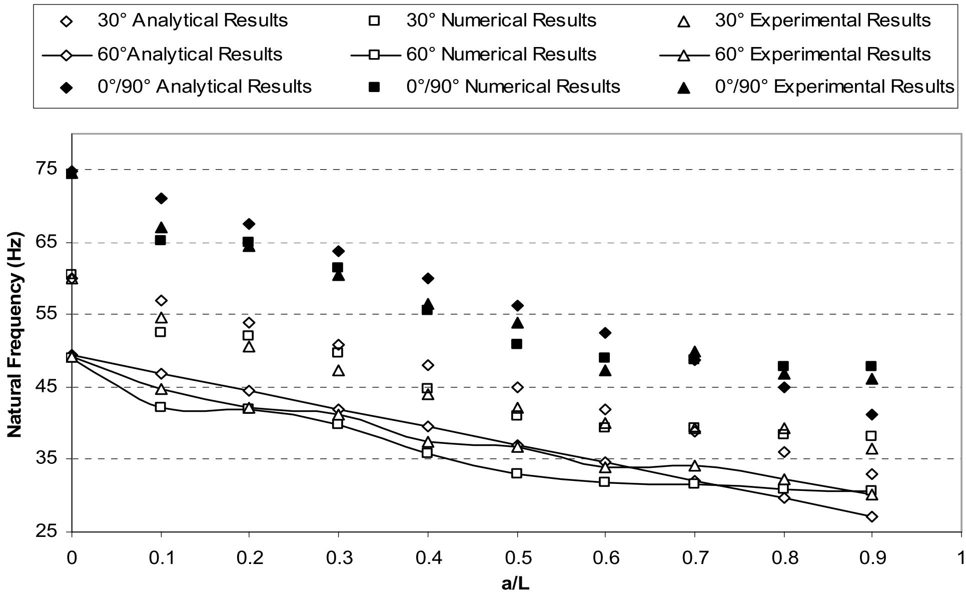

Figure 12. Changes in frequency with delamination for composite beam with single-edge delaminations for clamped–clamped boundary condition.

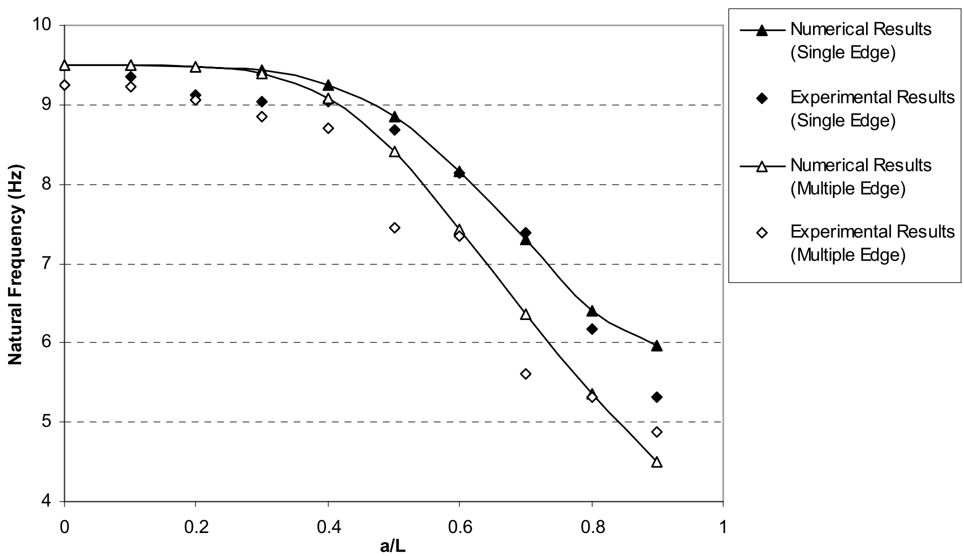

Figure 13. Variations of the relative frequency of $[30°]_{16}$ composite beam with both single and multiple-edge delaminations for clamped–free boundary condition.

having angle-ply of $[\theta]_{16}$ are lower than the others. Thus, it is seen that the effects of the stacking sequence of the beam are crucial when natural frequency values are taken into consideration. In fact, the frequency values of the beams composed of

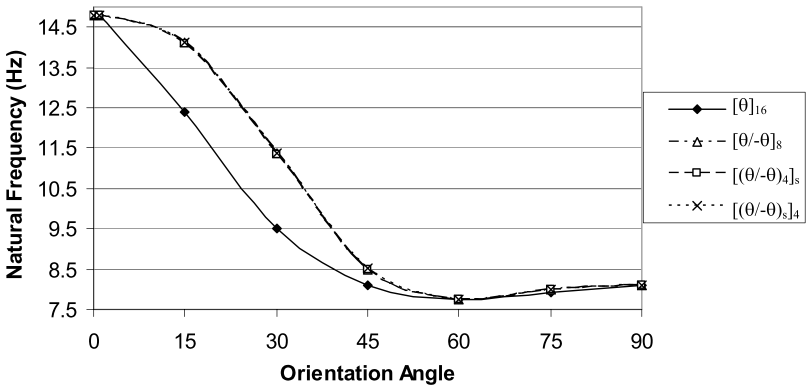

Figure 14. Variations of the relative frequency of composite beam with single edge delaminations ($a/L = 0.10$) for clamped–free boundary condition.

0° and the greater angles after 60° are equal to each other for all of the stacking sequences. The maximum frequency value is obtained for the beam consisted of 0° angle whereas the minimum frequency value is obtained for the beam having approximately 60° angle. When the variations of the frequencies in the beams of cross-plies are compared for $a/L = 0.1$, the frequency values of the beam having cross-ply $[0°/90°]_{4s}$ are found to be the highest (12.636 Hz) according to those of cross-plies $[(0°/90°)_s]_4$ (12.206 Hz) and $[0°/90°]_8$ (12.036 Hz).

4. Conclusion

This study shows the effects of location, size and number of delaminations, boundary conditions, orientation angles and stacking sequences on natural frequency of the laminated composite beam or plate. To this end, this work deals with the numerical, analytical and experimental natural frequency calculations of the delaminated composite clamped–clamped and clamped–free beams. The following conclusions can be drawn:

1. Single and multiple (two), edge and middle delaminations affect the natural frequency of laminated composite beams. In other words, the natural frequencies decrease when size and number of delaminations on the beam increase.
2. The frequency values in beams that have single-middle delamination are generally higher than those in beams that have single-edge delamination.
3. The frequency values of the beam with multiple-edge delamination are lower than those of the beams with single-edge delamination for all (a/L) ratios. The variations of the values are approximately parallel to each other.
4. The variations of the frequency values in the beams that have multiple-middle delamination and the multiple-edge delamination are approximately the same as those with the single-middle and single-edge delaminations.

5. The frequency value of the cross-ply beam of $[0°/90°]_{4s}$ is seen to be the highest amongst the ones with the angle-ply beam of $[\theta°]_{16}$.
6. If the stacking sequences are chosen as $[\theta]_{16}$, $[\theta/-\theta]_8$, $[(\theta/-\theta)_4]_s$ and $[(\theta/-\theta)_s]_4$, the maximum frequency value is obtained for a beam of angle 0° whereas the minimum frequency value is obtained for a beam of angle 60°.
7. When the variations of the frequencies in the beams of cross-plies are compared with each other for $a/L = 0.1$, the frequency values of the beam having cross-ply $[0°/90°]_{4s}$ are found to be the highest with respect to those of cross-plies $[(0°/90°)_s]_4$ and $[0°/90°]_8$.
8. The frequency values obtained from the numerical and experimental results for a beam with clamped–free boundary condition and multiple-edge delamination decrease very much with respect to the those with single-edge delamination after the a/L ratio is about 0.3.
9. As expected, the frequency values of the beams having clamped–clamped boundary conditions are higher than those of the beams having clamped–free boundary conditions.

Acknowledgements

The authors would like to thank Pamukkale University Scientific Research Council and Yonca-Onuk JV, Istanbul, for supporting this study under Project Contract No. 2008FBE008.

References

1. R. M. Jones, *Macromechanical Behavior of a Lamina Mechanics of Composite Materials*, 2nd edn. Taylor and Francis, Philadelphia, PA, USA (1999).
2. J. R. Vinson and R. L. Sierakowski, *The Behavior of Structures Composed of Composite Materials*, 2nd edn. Kluwer Academic Publishers, Secaucus, NJ (2002).
3. R. F. Gibson, *Principles of Composite Material Mechanics*. Taylor and Francis, Philadelphia, PA, USA (1994).
4. K. Alnefaie, Finite element modeling of composite plates with internal delamination, *Compos. Struct.* **90**, 21–27 (2009).
5. G. S. Ramtekkar, Free vibration analysis of delaminated beams using mixed finite element model, *J. Sound Vibr.* **328**, 428–440 (2009).
6. M. Palacz, M. Krawczuk and W. Ostachowicz, The spectral finite element model for analysis of flexural shear coupled wawe propagation. Part 2: Delaminated multilayer composite beam, *Compos. Struct.* **68**, 45–51 (2005).
7. D. Chakraborty, Artificial neural network based delamination prediction in laminated composites, *Mater. Design* **26**, 1–7 (2005).
8. A. Kumar and R. P. Shrivastava, Free vibration of square laminates with delamination around a central cutout using HSDT, *Compos. Struct.* **70**, 317–333 (2005).

9. A. G. Radu and A. Chattopadhyay, Dynamic stability analysis of composite plates including delaminations using a higher order theory and transformation matrix approach, *Int. J. Solids Struct.* **39**, 1949–1965 (2002).
10. H. Luo and S. Hanagud, Dynamics of delaminated beams, *Int. J. Solids Struct.* **37**, 1501–1519 (2000).
11. C. N. Della and D. Shu, Free vibration analysis of multiple delaminated beams under axial compressive load, *J. Reinf. Plast. Compos.* **28**, 1365–1380 (2009).
12. C. N. Della and D. Shu, Vibration of beams with two overlapping delaminations in prebuckled states, *Composites Part B: Eng.* **38**, 109–118 (2007).
13. S. K. Kim, A. Chattopadhyay and A. Ghoshal, Characterization of delamination effect on composite laminates using a new generalized layerwise approach, *Compos. Struct.* **81**, 1555–1566 (2003).
14. S. Lee, T. Park and G. Z. Voyiadjis, Vibration analysis of multi delaminated beams, *Composites Part B: Eng.* **34**, 647–659 (2003).
15. J. Lee, Free vibration analysis of delaminated composite beams, *Compos. Struct.* **74**, 121–129 (2000).
16. M. Topcu, G. Atlihan, H. Callioglu and E. S. Conkur, Stacking sequence effects on natural frequency of laminated composite beams, *Adv. Compos. Lett.* **17**, 7–13 (2008).
17. G. Atlihan, H. Callioglu, E. S. Conkur, M. Topcu and U. Yucel, Free vibration analysis of the laminated composite beams by using DQM, *J. Reinf. Plast. Compos.* **28**, 881–892 (2009).
18. G. Atlıhan, E. Demir, Z. Girgin and H. Çallıoğlu, Free vibration and buckling analysis of the laminated composite beams by using GDQM, *Adv. Compos. Lett.* **18**, 37–44 (2009).
19. W. T. Thomson, *Theory of Vibration with Application*, 4th edn. Prencice Hall, Englewood Cliffs, NJ, USA (1993).
20. ANSYS 10.0 User's Manual (2005).
21. N. Hu, H. Fukunaga, M. Kameyama, Y. Aramaki and F. K. Chang, Vibration analysis of delaminated composite beams and plates using a higher order finite element, *Int. J. Mech. Sci.* **44**, 1479–1503 (2002).
22. N. Hu, Buckling analysis of delaminated laminates with consideration of contact in buckling mode, *Int. J. Numer. Meth. Eng.* **10**, 1457–1479 (1994).
23. N. Hu, H. Sekine, H. Fukunaga and Z. Yao, Impact analysis of composite laminates with multiple delaminations, *Intl. J. Imp. Eng.* **22**, 633–648 (1999).
24. H. Luo and S. Hanagud, Dynamics of delaminated beams, *Int. J. Solids Struct.* **37**, 1501–1519 (2000).
25. M. H. H. Shen and J. E. Grady, Free vibrations of delaminated beams, *AIAA J.* **30**, 1361–1370 (1992).
26. G. Atlihan, Vibration analysis of the delaminated composite beams, *PhD Thesis*, Department of Mechanical Engineering, University of Pamukkale, Denizli, TR (2010).